



Iodide-ion conduction in methylammonium lead iodide perovskite: some extraordinary aspects

 Roger A. De Souza * and Denis Barboni

 Cite this: *Chem. Commun.*, 2019, 55, 1108

 Received 20th November 2018,
Accepted 2nd January 2019

DOI: 10.1039/c8cc09236b

rsc.li/chemcomm

A recent model of iodide-ion conduction in methylammonium lead iodide perovskite ($\text{CH}_3\text{NH}_3\text{PbI}_3$) is discussed. Issues include the low activation barrier of vacancy migration and the high diffusivities of iodine vacancies and interstitials. Comparisons are also made with the behaviour of point defects in the oxide perovskite SrTiO_3 .

In hindsight, it is hardly surprising that the outstanding photovoltaic material methylammonium lead iodide ($\text{CH}_3\text{NH}_3\text{PbI}_3 = \text{MAPbI}_3$)¹—a hybrid organic–inorganic perovskite—is characterised by highly mobile anions.^{2–4} Impressively high oxide-ion conductivity is found in numerous ABO_3 oxide perovskites;^{5–9} X^- anions are mobile in halide ABX_3 perovskites;^{10–17} and high Li^+ conductivity is displayed by Li_3OCl and similar anti-perovskite compounds,^{18–21} in which Li^+ resides on the same crystallographic site as O^{2-} and X^- in the oxide and halide perovskites. Iodide-ion conduction in MAPbI_3 , therefore, is not unprecedented; it is marked, however, by some surprises.

One surprise is the excessive scatter in activation enthalpies reported for ion transport in MAPbI_3 (see Fig. 1).^{4,22–45} Values determined experimentally^{4,22–35} range between 0.1 eV and 0.7 eV, with higher values, it seems, being observed at higher temperatures. Another surprise discernable in Fig. 1 is the limited help provided by computational studies^{35–44} in understanding experimental data. Certainly, predicted activation enthalpies for iodine-vacancy migration (0.08 eV to 0.58 eV) are generally lower than those for MA-vacancy migration (0.46 eV to 1.18 eV), but beyond this, there is little to be deduced. Indeed, the wide range of computational values guarantees that there is one value sufficiently close to a given experimental value. Solid state diffusion experiments are notoriously difficult to perform accurately and interpret correctly, but it is highly unlikely that experimental inaccuracies or artefacts are responsible for all the scatter observed.

In a recent study,⁴⁶ we demonstrated that a single model with one set of parameters could explain quantitatively diverse experimental data^{4,23,29,32,33} related to ion conduction in MAPbI_3 . The model combines knowledge of the jump rate of iodine vacancies with the results of defect chemical modelling. It requires (a) iodine ions to migrate by a vacancy mechanism over an activation barrier of $\Delta H_{\text{mig,v}} = 0.08$ eV; and (b) the concentration of iodine vacancies to be fixed at low temperatures by acceptor dopants ($c_v = c_a$), but to vary at higher temperatures, on account of anti-Frenkel disorder generating vacancies and interstitials becoming dominant ($c_v = c_i$). This explanation raises several questions. This communication is devoted to the discussion of these questions.

Origin of scatter: an alternative illustration. The transition in defect behaviour, from extrinsic to intrinsic, is shown exemplarily for four different values of c_a in Fig. 2(a). From these data the iodide-ion conductivity [Fig. 2(b)] can be calculated with

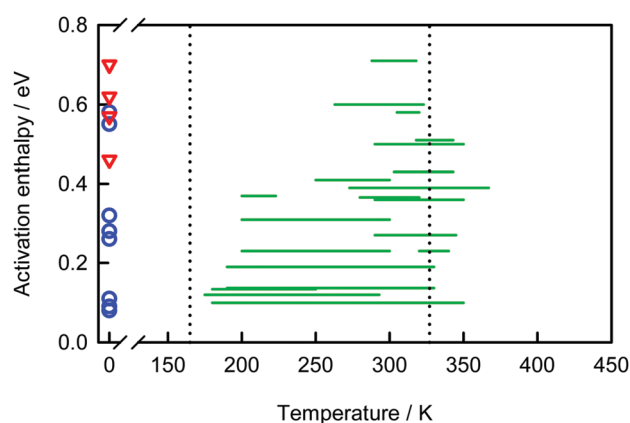


Fig. 1 Activation enthalpies reported in the literature for ion transport in MAPbI_3 . Experimental data, shown as green lines, are plotted against the temperature range over which the data was acquired. Computational data, referring to migration barriers obtained in static atomistic calculations, are plotted at zero K (red triangles, MA-vacancy migration; blue circles, iodine-vacancy migration). The vertical dotted lines indicate the phase-transition temperatures: orthorhombic–tetragonal and tetragonal–cubic.

Institute of Physical Chemistry, RWTH Aachen University, 52056 Aachen, Germany.
E-mail: desouza@pc.rwth-aachen.de; Fax: +49 241 80 92128;
Tel: +49 241 80 94739

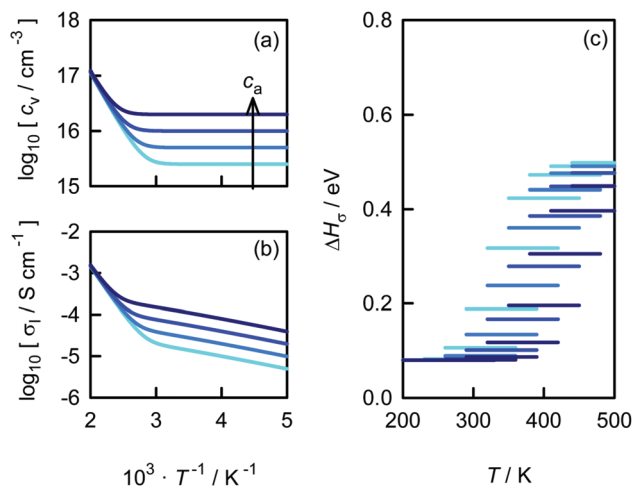


Fig. 2 Model of ion conduction in MAPbI₃.⁴⁶ (a) concentration of iodine vacancies as a function of reciprocal temperature for various acceptor concentrations; (b) iodide-ion conductivity as a function of reciprocal temperature; (c) effective activation energies over 100 K intervals obtained from the data in (b).

knowledge of the iodine-vacancy mobility.⁴⁶ And subsequently, effective activation enthalpies of conduction can be obtained over rolling intervals of 100 K according to $\Delta H_{\sigma} = -k_B(\partial \ln \sigma_I / \partial T^{-1})$; the results are plotted in Fig. 2(c). Comparing this plot with Fig. 1, we recognise, first, that a significant amount of scatter may come from researchers performing experiments over small ranges in temperatures on samples of varying c_a and being unaware of the transition in defect behaviour. And second, that experimental activation enthalpies higher than 0.5 eV cannot refer to iodide-ion transport in bulk MAPbI₃. If inaccuracies and artefacts can be ruled out, one has to conclude that either a different transport path (e.g. along grain boundaries), a different mobile ion (e.g. MA⁺)^{24,26,31,47} or a different physical process is being probed.

The activation enthalpy of iodine-vacancy migration. At first sight, an activation barrier of 0.08 eV seems far too small for the migration of an ion through a polar solid. A deeper look is possibly afforded by examining for comparison data for other perovskite systems. We stress that it is $\Delta H_{\text{mig},v}$ that is required, not ΔH_{σ} or similar (cf. Fig. 2).

Thus, of the various classes of perovskites in which ion migration has been examined, the ABO₃ compounds constitute the most well characterised. They exhibit activation enthalpies of oxygen-vacancy migration in the range of 0.5 eV to 1.5 eV.^{6–9} For the class of ABX₃ halide perovskites, reported values of $\Delta H_{\text{mig},v}$ for the migration of X[–] = F[–], Cl[–] or Br[–] are between 0.25 eV and 0.54 eV.^{11–14} One exception is the activation enthalpy of only 0.11 eV obtained by Bouznik *et al.*¹⁰ for F[–] migration in CsPbF₃, but this result requires confirmation: the closely related compounds, CsPbCl₃ and CsPbBr₃, show much higher values of 0.29 eV and 0.25 eV.¹² The other class of perovskites with singly charged ions is the class of anti-perovskites, such as Li₃OCl (with mobile Li⁺). Here, experimental and computational studies reliably return $\Delta H_{\text{mig},v}$ between 0.26 eV and 0.37 eV.^{18–21} Evidently, singly charged ions, residing on a specific crystallographic site in the perovskite structure, migrate with substantially lower

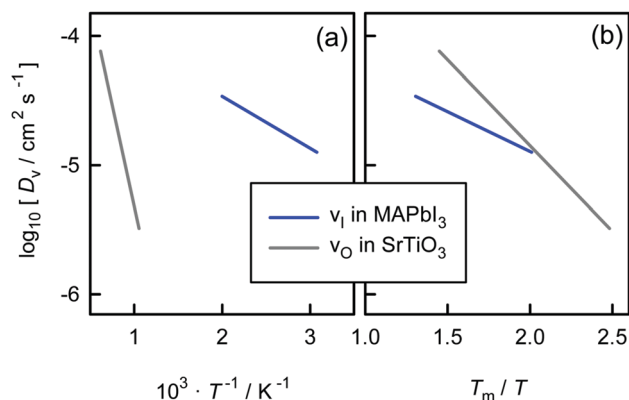


Fig. 3 Comparison of anion-vacancy diffusion coefficients in MAPbI₃ and SrTiO₃.^{46,54} (a) versus reciprocal temperature (b) versus reciprocal homologous temperature.

activation barriers than doubly charged ions. This emphasises the contribution of Coulomb interactions to the migration barrier.⁴⁸ Data for X[–] or Li⁺ migration thus provide a closer comparison than data for oxide-ion migration. Nevertheless, the value of 0.08 eV predicted by us⁴⁶ and others^{38,43} for $\Delta H_{\text{mig},v}$ in MAPbI₃ remains remarkably low.

Perhaps this is not quite the right approach. Perhaps a better approach is to identify whether some factor exclusive to MAPbI₃ is responsible for the low $\Delta H_{\text{mig},v}$. Ion conduction has been investigated in perovskites that contain Pb²⁺ with its lone pair; that include more covalent moieties (Br[–]) as opposed to the more ionic F[–] or Li⁺; or that have large lattice constants: and in all cases, the activation barriers of migration are above 0.25 eV. We attribute the low value of $\Delta H_{\text{mig},v}$, therefore, to the MA⁺ cation. Specifically, we suggest that the temporary alignment of adjacent MA⁺ cations in the cubic phase allows iodide ions to hop to adjacent vacant sites over low activation barriers.⁴⁹ Whether the migration dynamics of iodide ions are coupled to the rotational dynamics of the MA⁺ cations, possibly even giving rise to migration in the sense of a paddle-wheel mechanism,⁵⁰ remains to be elucidated. The activation barriers

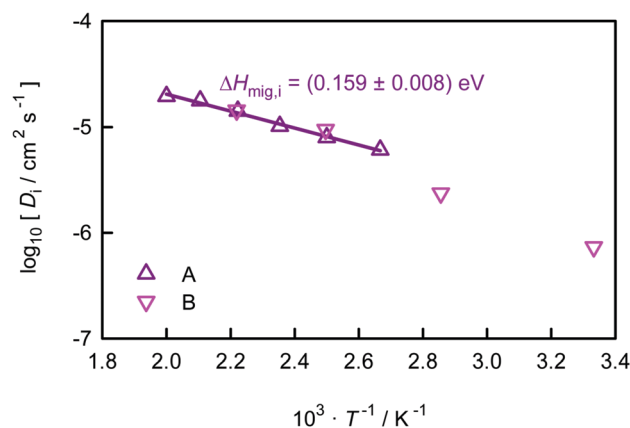


Fig. 4 Diffusion coefficient of iodine interstitials in MAPbI₃ versus reciprocal temperature. Data obtained from MD simulations: A, this study; B, Delugas *et al.*⁴⁰

Table 1 Comparison of point-defect enthalpies and entropies reported in the literature for MAPbI₃ and SrTiO₃

	MAPbI ₃	SrTiO ₃	Ref.	
$\Delta H_{\text{mig,v}}/\text{eV}$	(0.080 ± 0.004), 0.08, 0.09	0.62	46, 38 and 43	55 and 56
$\Delta S_{\text{mig,v}}/k_{\text{B}}$	−(3.4 ± 0.1)	−(0.53 ± 0.70)	46	55
$\Delta H_{\text{mig,i}}/\text{eV}$	(0.159 ± 0.008), 0.19, 0.08, 0.08	0.3, 0.4, 1.34, 1.25	This study, 39, 38 and 43	63, 63, 62 and 64
$\Delta S_{\text{mig,i}}/k_{\text{B}}$	−(0.7 ± 0.2)		This study	
$\Delta H_{\text{Sch}}/\text{eV}$	0.16	2.5	65	66
$\Delta S_{\text{Sch}}/k_{\text{B}}$		−1.04		66
$\Delta H_{\text{aF}}/\text{eV}$	(0.85 ± 0.05), 0.82	8.3, 8.36	46 and 41	62 and 67
$\Delta S_{\text{aF}}/k_{\text{B}}$	−(3.45 ± 0.05)		46	

for MA⁺ re-orientation in cubic MAPbI₃ are 60–100 meV,^{51–54} *i.e.* of comparable magnitude to $\Delta H_{\text{mig,v}}$ (= 80 meV).

The diffusivity of iodine vacancies. In order to establish whether the calculated diffusivity of iodine vacancies in MAPbI₃ [obtained from molecular dynamics (MD) simulations⁴⁶] is unreasonably high, possibly on account of the low $\Delta H_{\text{mig,v}}$, we compare in Fig. 3(a) the calculated values with the corresponding data for oxygen vacancies in SrTiO₃ [taken from experiment;⁵⁵ MD data⁵⁶ are very similar]. We find that the absolute values are comparable for the two materials [$D_{\text{v}} \sim 10^{-(5\pm 1)} \text{ cm}^2 \text{ s}^{-1}$], albeit over vastly different temperature ranges. This difference in temperatures is not unexpected, however, for the two materials exhibit vastly different melting points: $T_{\text{m}} = 650 \text{ K}$ for MAPbI₃;⁵⁷ $T_{\text{m}} = 2350 \text{ K}$ for SrTiO₃.⁵⁸ We take account of this difference by using the homologous temperature T/T_{m} .⁵⁹ Hence, plotting the same D_{v} data against the reciprocal homologous temperature in Fig. 3(b), we find close agreement between the two datasets. The diffusivity of anion vacancies in MAPbI₃ is, evidently, physically reasonable. Consequently, the low value of $\Delta H_{\text{mig,v}}$ appears indirectly to be physically reasonable, too.

The diffusivity of iodine interstitials. In order to reproduce experimental conductivity data,^{4,23,29,32,33} we required⁴⁶ only iodine vacancies to be mobile. Iodine interstitials have to be substantially less mobile than iodine vacancies (*i.e.* $D_{\text{i}} < D_{\text{v}}$), since in the intrinsic regime $c_{\text{v}} = c_{\text{i}}$. Although $D_{\text{i}}(T)$ for MAPbI₃ has already been predicted by Delugas *et al.*⁴⁰ by means of MD simulations with the MYP potentials,⁶⁰ their MD data for the two lowest (of four) temperatures examined suffer, it would appear, from poor statistics. Consequently, we re-examined the issue, employing the same MYP potentials⁶⁰ but a much larger simulation cell (4000 f.u. *vs.* 256 f.u.) and a larger number of interstitials (12 *vs.* 1), to improve the statistics.

In our simulations (with the LAMMPS code⁶¹) we monitored the evolution of the iodide ions' mean-square-displacement as a function of time, from which we obtained iodine tracer diffusion coefficients (not shown). These we converted into interstitial diffusivities assuming three-dimensional diffusion and a tracer correlation coefficient for interstitial migration of unity. The interstitial diffusivities that we obtained are compared with the published data of Delugas *et al.*⁴⁰ in Fig. 4. Our results agree very well with the published data at higher temperatures and indicate a clear discrepancy for the two lowest temperatures. The data of Fig. 3 and 4, taken together, confirm that $D_{\text{i}} < D_{\text{v}}$ up to $T = 500 \text{ K}$.

According to our data, the activation enthalpy of iodine-interstitial migration in MAPbI₃ is $\Delta H_{\text{mig,i}} = (159 \pm 8) \text{ meV}$.

As can be gathered from Fig. 4, Delugas *et al.*⁴⁰ obtained a much higher value (of 240 meV). Interestingly, density-functional-theory (DFT) calculations^{38,43} predict $\Delta H_{\text{mig,i}} \approx \Delta H_{\text{mig,v}} \approx 80 \text{ meV}$ (see Table 1). Why DFT calculations yield values for $\Delta H_{\text{mig,v}}$ similar to our MD value⁴⁶ but values for $\Delta H_{\text{mig,i}}$ much lower than our MD value (this study) remains to be clarified. For SrTiO₃, $\Delta H_{\text{mig,i}}$ is predicted to be either slightly lower or substantially higher than $\Delta H_{\text{mig,v}}$ (see Table 1), whereas for perovskite KMnF₃, $\Delta H_{\text{mig,i}} < \Delta H_{\text{mig,v}}$ is predicted.^{11,13} A universal rule for all perovskites regarding the two activation enthalpies is, therefore, not apparent at present.

aF vs. Sch. We ascribed⁴⁶ the dominance of anti-Frenkel disorder over (MA)I-partial Schottky disorder in MAPbI₃ to a huge, negative entropy of Schottky disorder (*e.g.* $\Delta S_{\text{Sch}} = -30k_{\text{B}}$). Such an extreme value arises, we suggest here, from the loss of rotational freedom that the MA⁺ cations surrounding an MA vacancy experience, on account of the cations' correlated rotational dynamics. In order to emphasise the unusualness of MAPbI₃, here we also calculate (from enthalpies and entropies) a critical temperature T_{d} above which anti-Frenkel rather than Schottky disorder will dominate an undoped perovskite's defect chemistry [T_{d} is shifted upwards by sufficient acceptor doping, see Fig. 2(b)]. Thus, with $\Delta S_{\text{Sch}} = -30k_{\text{B}}$, the critical temperature is *ca.* 290 K, *i.e.* $T_{\text{d}}/T_{\text{m}} = 0.45$. In contrast, for SrTiO₃, even with (a grossly overestimated) $\Delta S_{\text{aF}} = +20k_{\text{B}}$, we find $T_{\text{d}}/T_{\text{m}} > 1$, *i.e.* SrTiO₃ melts before anti-Frenkel disorder can dominate.

Funding from German Research Foundation (DFG) within the framework of the collaborative research centre SFB917, "Nanoswitches", is acknowledged. Simulations were performed with computing resources granted by RWTH Aachen University under project thes0333. C. L. Freeman, A. Walsh and D. L. Irving are thanked for helpful discussions.

Conflicts of interest

There are no conflicts to declare.

Notes and references

- 1 A. Kojima, K. Teshima, Y. Shirai and T. Miyasaka, *J. Am. Chem. Soc.*, 2009, **131**, 6050; M. A. Green, A. Ho-Bailie and H. J. Snaith, *Nat. Photonics*, 2014, **8**, 506; M. Saliba, J. P. Correa-Baena, M. Grätzel, A. Hagfeldt and A. Abate, *Angew. Chem., Int. Ed.*, 2018, **57**, 2554.
- 2 A. Dualeh, T. Moehl, N. Tétreault, J. Teuscher, P. Gao, M. K. Nazeeruddin and M. Grätzel, *ACS Nano*, 2013, **8**, 362.
- 3 Z. Xiao, Y. Yuan, Y. Shao, Q. Wang, Q. Dong, C. Bi, P. Sharma, A. Gruverman and J. Huang, *Nat. Mater.*, 2015, **14**, 193.

- 4 T. Y. Yang, G. Gregori, N. Pellet, M. Grätzel and J. Maier, *Angew. Chem., Int. Ed.*, 2015, **54**, 7905.
- 5 T. Ishigaki, S. Yamauchi, K. Kishio, J. Mizusaki and K. Fueki, *J. Solid State Chem.*, 1988, **73**, 179; J. Mizusaki, *Solid State Ionics*, 1992, **52**, 79.
- 6 M. Cherry, M. S. Islam and C. R. A. Catlow, *J. Solid State Chem.*, 1995, **118**, 125; M. S. Islam, *J. Mater. Chem.*, 2000, **10**, 1027; T. T. Mayeshiba and D. D. Morgan, *Solid State Ionics*, 2016, **296**, 71.
- 7 J. B. Goodenough, *Rep. Prog. Phys.*, 2004, **67**, 1915.
- 8 *Perovskite Oxide for Solid Oxide Fuel Cells*, ed. T. Ishihara, Springer, 2009.
- 9 R. A. De Souza, *Adv. Funct. Mater.*, 2015, **25**, 6326.
- 10 V. M. Bouznik, Yu. N. Moskvich and V. N. Voronov, *Chem. Phys. Lett.*, 1976, **37**, 464.
- 11 J. A. Kilner, *Philos. Mag. A*, 1981, **43**, 1473.
- 12 J. Mizusaki, K. Arai and K. Fueki, *Solid State Ionics*, 1983, **11**, 203.
- 13 R. R. Becher, M. J. L. Sangster and D. Strauch, *J. Phys.: Condens. Matter*, 1989, **1**, 7801.
- 14 R. E. Boyett, M. G. Ford and P. A. Cox, *Solid State Ionics*, 1995, **81**, 61.
- 15 A. V. Chadwick, J. H. Strange, G. A. Ranieri and M. Terenzi, *Solid State Ionics*, 1983, **9–10**, 555; D. Z. Demetriou, C. R. A. Catlow, A. V. Chadwick, G. J. McIntyre and I. Abrahams, *Solid State Ionics*, 2005, **176**, 1571.
- 16 N. H. Anderson, J. K. Kjemis and W. Hayes, *Solid State Ionics*, 1985, **17**, 143; R. L. Narayan and S. V. Suryanarayana, *Mater. Lett.*, 1991, **11**, 305; T. A. Kuku, *Thin Solid Films*, 1998, **325**, 246.
- 17 K. Yamada, K. Isobe, E. Tsuyama, T. Okuda and Y. Furukawa, *Solid State Ionics*, 1995, **79**, 152; K. Yamada, K. Isobe, T. Okuda and Y. Furukawa, *Z. Naturforsch., A: Phys. Sci.*, 1994, **49**, 258.
- 18 G. Schwing, A. Hönnerscheid, L. van Wüllen and M. Jansen, *ChemPhysChem*, 2003, **4**, 343.
- 19 Y. Zhao and L. L. Daemen, *J. Am. Chem. Soc.*, 2012, **134**, 15042.
- 20 A. Emly, E. Kioupakis and A. Van der Ven, *Chem. Mater.*, 2013, **25**, 4663.
- 21 J. A. Dawson, H. Chen and M. S. Islam, *J. Phys. Chem. C*, 2018, **122**, 23978.
- 22 O. Knop, R. E. Wasylshen, M. A. White, T. S. Cameron and M. J. M. V. Oort, *Can. J. Chem.*, 1990, **68**, 412.
- 23 Y. Yuan, J. Chae, Y. Shao, Q. Wang, Z. Xiao, A. Centrone and J. Huang, *Adv. Energy Mater.*, 2015, **5**, 1.
- 24 M. Bag, L. A. Renna, R. Y. Adhikari, S. Karak, F. Liu, P. M. Lahti, T. P. Russell, M. T. Tuominen and D. Venkataraman, *J. Am. Chem. Soc.*, 2015, **137**, 13130.
- 25 D. Bryant, S. Wheeler, B. C. O'Regan, T. Watson, P. R. Barnes, D. Worsley and J. Durrant, *J. Phys. Chem. Lett.*, 2015, **6**, 3190.
- 26 L. Contreras, J. A. Idigoras, A. Todinova, M. Salado, S. Kazim, S. Ahmad and J. Anta, *Phys. Chem. Chem. Phys.*, 2016, **18**, 31033.
- 27 H. Yu, H. Lu, F. Xie, S. Zhou and N. Zhao, *Adv. Funct. Mater.*, 2016, **26**, 1411.
- 28 C. Li, S. Tscheuschner, F. Paulus, P. E. Hopkinson, J. Kießling, A. Köhler, Y. Vaynzof and S. Huettner, *Adv. Mater.*, 2016, **28**, 2446.
- 29 D. W. deQuilettes, W. Zhang, V. M. Burlakov, D. J. Graham, T. Leijtens, V. Oshero, A. Bulovic, H. J. Snaith, D. S. Ginger and S. D. Stranks, *Nat. Commun.*, 2016, **7**, 11683.
- 30 J. Xing, Q. Wang, Q. Dong, Y. Yuan, Y. Fang and J. Huang, *Phys. Chem. Chem. Phys.*, 2016, **18**, 30484.
- 31 M. N. F. Hoque, N. Islam, Z. Li, G. Ren, K. Zhu and Z. Fan, *ChemSusChem*, 2016, **9**, 2692.
- 32 Y. Zhao, W. Zhou, X. Zhou, K. Liu, D. Yu and Q. Zhao, *Light: Sci. Appl.*, 2017, **6**, e16243.
- 33 O. S. Game, G. J. Buchsbaum, Y. Zhou, N. P. Padture and A. I. Kingon, *Adv. Funct. Mater.*, 2017, **27**, 1606584.
- 34 X. Guan, W. Hu, M. A. Haque, N. Wei, Z. Liu, A. Chen and T. Wu, *Adv. Funct. Mater.*, 2017, **28**, 1704665.
- 35 S. Meloni, T. Moehl, W. Tress, M. Franckeviius, M. Saliba, Y. H. Lee, P. Gao, M. K. Nazeeruddin, S. M. Zakeeruddin, U. Rothlisberger and M. Graetzel, *Nat. Commun.*, 2016, **7**, 10334.
- 36 C. Eames, J. M. Frost, P. R. F. Barnes, B. C. O'Regan, A. Walsh and M. S. Islam, *Nat. Commun.*, 2015, **6**, 7497.
- 37 J. Haruyama, K. Sodeyama, L. Han and Y. Tateyama, *J. Am. Chem. Soc.*, 2015, **137**, 10048.
- 38 J. M. Azpiroz, E. Mosconi, J. Bisquert and F. De Angelis, *Energy Environ. Sci.*, 2015, **8**, 2118.
- 39 D. Yang, W. Ming, H. Shi, L. Zhang and M. H. Du, *Chem. Mater.*, 2016, **28**, 4349.
- 40 P. Delugas, C. Caddeo, A. Filippetti and A. Mattoni, *J. Phys. Chem. Lett.*, 2016, **7**, 2356.
- 41 E. Mosconi, D. Meggiolaro, H. J. Snaith, S. D. Stranks and F. De Angelis, *Energy Environ. Sci.*, 2016, **8**, 3180.
- 42 J. H. Yang, W. J. Yin, J. S. Park and S. H. Wei, *J. Mater. Chem. A*, 2016, **4**, 13105.
- 43 D. Meggiolaro, E. Mosconi and F. De Angelis, *ACS Energy Lett.*, 2018, **3**, 447.
- 44 U.-G. Jong, C.-J. Yu, G.-C. Ri, A. P. McMahan, N. M. Harrison, P. R. F. Barnes and A. Walsh, *J. Mater. Chem. A*, 2018, **6**, 1067.
- 45 D. A. Egger, L. Kronik and A. M. Rappe, *Angew. Chem., Int. Ed.*, 2015, **54**, 12437.
- 46 D. Barboni and R. A. De Souza, *Energy Environ. Sci.*, 2018, **11**, 3266.
- 47 A. Senocrate, I. Moudrakovski, G. Y. Kim, T.-Y. Yang, G. Gregori, M. Grätzel and J. Maier, *Angew. Chem., Int. Ed.*, 2017, **56**, 7755.
- 48 J. P. Parras, A. R. Genreith-Schriever, H. Zhang, M. T. Elm, T. Norby and R. A. De Souza, *Phys. Chem. Chem. Phys.*, 2018, **20**, 8008.
- 49 C.-J. Tong, W. Geng, O. V. Prezhdo and L.-M. Liu, *ACS Energy Lett.*, 2017, **2**, 1997.
- 50 M. Jansen, *Angew. Chem., Int. Ed.*, 1991, **30**, 1547.
- 51 T. Chen, B. J. Foley, B. Ipek, M. Tyagi, J. R. Copley, C. M. Brown, J. J. Choi and S. H. Lee, *Phys. Chem. Chem. Phys.*, 2015, **17**, 31278.
- 52 J. S. Bechtel, R. Seshadri and A. Van der Ven, *J. Phys. Chem. C*, 2016, **120**, 12403.
- 53 D. H. Fabini, T. A. Siaw, C. C. Stoumpos, G. Laurita, D. Olds, K. Page, J. G. Hu, M. G. Kanatzidis, S. Han and R. Seshadri, *J. Am. Chem. Soc.*, 2017, **139**, 16875.
- 54 J. Lahnsteiner, G. Kresse, J. Heinen and M. Bokdam, *Phys. Rev. Mater.*, 2018, **2**, 073604.
- 55 R. A. De Souza, V. Metlenko, D. Park and T. E. Weirich, *Phys. Rev. B: Condens. Matter Mater. Phys.*, 2012, **85**, 174109.
- 56 S. P. Waldow and R. A. De Souza, *ACS Appl. Mater. Interfaces*, 2016, **8**, 12246.
- 57 B. Brunetti, C. Cavallo, A. Cicciolo, G. Gigli and A. Latini, *Sci. Rep.*, 2016, **6**, 31896.
- 58 J. A. Basmajian and R. C. DeVries, *J. Am. Ceram. Soc.*, 1957, **40**, 373.
- 59 A. M. Brown and M. F. Ashby, *Acta Metall.*, 1980, **28**, 1085.
- 60 A. Mattoni, A. Filippetti, M. I. Saba and P. Delugas, *J. Phys. Chem. C*, 2015, **119**, 17421.
- 61 S. J. Plimpton, *J. Comput. Phys.*, 1995, **117**, 1.
- 62 J. Crawford and P. Jacobs, *J. Solid State Chem.*, 1999, **144**, 423.
- 63 B. P. Uberuaga and L. J. Vernon, *Solid State Ionics*, 2013, **253**, 18.
- 64 A. Samanta, W. E and S. B. Zhang, *Phys. Rev. B: Condens. Matter Mater. Phys.*, 2012, **86**, 195107.
- 65 A. Walsh, D. O. Scanlon, S. Chen, X. G. Gong and S. H. Wei, *Angew. Chem., Int. Ed.*, 2015, **54**, 1791.
- 66 R. Moos and K.-H. Härdtl, *J. Am. Ceram. Soc.*, 1997, **80**, 2549.
- 67 J. N. Baker, P. C. Bowes, J. S. Harris and D. L. Irving, *J. Appl. Phys.*, 2018, **124**, 114101.